Slow Light in Molecular-Aggregate Nanofilms

E. Cabrera-Granado,[1,2] E. Díaz,[3,2] and Oscar G. Calderón[2]

[1]*Max Planck Institute for the Physics of Complex Systems, 01187 Dresden, Germany*
[2]*Universidad Complutense, E-28040 Madrid, Spain*
[3]*Institute for Materials Science, Technische Universität Dresden, 01062 Dresden, Germany*

(Received 19 January 2011; published 29 June 2011; corrected 27 February 2012)

We study slow-light performance of molecular aggregates arranged in nanofilms by means of coherent population oscillations. The molecular cooperative behavior inside the aggregate enhances the delay of input signals in the gigahertz range in comparison with other coherent population oscillation-based devices. Moreover, the problem of residual absorption present in coherent population oscillation processes is removed. We also propose an optical switch between different delays by exploiting the optical bistability of these aggregates.

DOI: 10.1103/PhysRevLett.107.013901 PACS numbers: 42.65.Pc, 78.67.Sc

The optical engineering of the speed of light plays an important role in the development of all-optical devices for telecommunications. Among the different mechanisms exploited to obtain slow light [1,2], coherent population oscillations (CPOs) deal with two-level systems and are feasible at room temperature [3,4]. It is worth mentioning that there is some controversy in this regard, since most of the experiments can also be explained by saturable absorption [5,6]. Being that the source spectral width is larger than the coherent hole of the absorption profile, some reasonable doubts are raised about the existence of *coherent* population oscillations. From a theoretical point of view, a rate-equation analysis does not distinguish between both processes, and a density-matrix formalism is required. To develop photonic applications, a large fractional delay (time delay normalized to the pulse length) is desirable in compact devices. Furthermore, bandwidths up to the gigahertz or terahertz range and a constrained distortion of the input pulses are needed to integrate slow-light mechanisms in communication networks nowadays. However, the delay decreases with the signal bandwidth, which makes it difficult to achieve these objectives. Moreover, the residual absorption present in CPO processes leads to a greatly diminished output intensity when longer delays are sought. In this work we propose a new optical CPO-based device considering nanofilms of linear aggregates of dye molecules, so-called J aggregates, which leads to a fractional delay up to 0.33 for 135-ps-long pulses while the ratio between the standard deviation of the output and input pulses reaches a value of 2. More interestingly, the signal modulation is amplified instead of absorbed, which establishes a clear signature to distinguish between CPO and saturable absorption processes in typical two-level systems, since in the latter no gain in the weak intensity modulation can be achieved. We also show how the already predicted optical bistability on J aggregates [7] can provide an all-optical switch between two well-differentiated time delays and pulse distortions. Remarkably J aggregates display narrow absorption bands redshifted with respect to those of the isolated molecules due to collective interaction, which leads to interesting optical phenomena studied in the past decade [8]. Because of disorder effects affecting these systems, only some of the molecules of the aggregate are coherently bound. In the most favorable situation, namely, at low temperatures, the number of molecules over which the excitation is localized is $\sim$100, although a real aggregate consists of thousands of individual molecules. In view of these properties, we consider J aggregates as modeled by an ensemble of inhomogeneously broadened two-level systems at low temperatures [7,9]. With regard to CPO processes, we study the response of an ultrathin film of oriented linear J aggregates to a strong pump field E_0 at frequency ω and two sidebands $E_{\pm 1}$ at frequencies $\omega \pm \delta$. Here δ is the beat frequency between fields. Because of disorder effects, the film can be considered as consisting of homogeneous aggregates of different coherent sizes N. By using the density-matrix formalism under the rotating wave and slowly varying amplitude in time approximations, we describe the state of a segment of size N as

$$\begin{aligned} \dot{\sigma}^N &= [i(\omega - \omega_{ba}^N) - 1/T_2]\sigma^N - id^N E Z^N/\hbar, \\ \dot{Z}^N &= i2d^N(\sigma^{N*}E - \sigma^N E^*)/\hbar - (Z^N + 1)/T_1^N. \end{aligned} \tag{1}$$

Here σ^N is the slowly varying in time coherence between the two levels which depends on the segment size N. The transition frequency and the dipole moment between the ground (a) and upper (b) energy levels of every segment read ω_{ba}^N and $d^N = d^1\sqrt{N}$, respectively. The superscript 1 refers to single-molecule properties. We assume field polarization directed along the transition dipole moments of all the aggregates, which in addition are parallel to each other as well as to the film plane. The relaxation time of the population inversion $Z^N = (\rho_{bb}^N - \rho_{aa}^N)$ due to spontaneous emission is $T_1^N = T_1^1/N$, while T_2 is related to other dephasing processes.

Field propagation in dense media can be described by means of an integral equation where the slowly varying approximation in time is considered but not in space [9]. For film thickness smaller than the optical wavelength, spatially homogeneous polarization can be assumed, which leads to the following field equation:

$$E = E^{\text{in}} + \frac{\mu_0 cL}{2} i\omega P, \tag{2}$$

where μ_0 is the permeability constant, c is the speed of light, and L is the film thickness. The incident field is $E^{\text{in}}(t) = E_0 + E_1 \exp(-i\delta t) + E_{-1}\exp(i\delta t)$. The second term accounts for the field created by the molecules polarized by the incident field. We checked the full propagation integral to raise the same results as Eq. (2) for films of tens of nanometers, a thickness achievable by the spin-coating technique [10]. Thus, for simplicity and to gain a deeper analytical insight, we will restrict ourselves to this case. Equation (2) resembles that found by Lu and Zhu, who proved that local field effects can improve the slow-light performance in a hybrid nanocrystal complex [11].

The polarization is calculated by considering the contributions of all coherent segments of different sizes: $P = N_0 \sum_N p(N) d^N \sigma^N$. Here N_0 is the density of localization segments, and $p(N)$ refers to the disorder distribution function over localization lengths. Note that the size dispersion of the coherent segments in the system results from the inhomogeneous broadening affecting the J band at low temperatures, which mainly gives rise to the fluctuation of transition energies $\hbar\omega_{ba}^N$. As in Ref. [7], we replace the average over sizes by one performed over the normalized detunings $\Delta^N = (\omega\text{-}\omega_{ba}^N)T_2$. The distribution $p(N)$ indeed can be accessible by absorption experiments and is considered as Gaussian-like hereafter:

$$\sum_N p(N) \sim \int_{-\infty}^{\infty} \frac{\exp(\frac{-(\Delta^N - \Delta_0)^2}{2G^2})}{\sqrt{2\pi G^2}} d\Delta^N, \tag{3}$$

$\Delta_0 = (\omega\text{-}\omega_0)T_2$ being the detuning between the incident frequency and the mean of the transition frequency distribution ω_0. The magnitude of the J bandwidth resulting from the inhomogeneous broadening is denoted by G in units of $1/T_2$. From now on, size dispersion effects are restricted to these detuning effects in our calculations, for the sake of simplicity. Thus, we will substitute the size-dependent quantities by their mean value in the aggregate and remove the index N, i.e., $T_1^N = T_1$ and $d^N = d$.

Similarly to Ref. [12], we treat Eqs. (1) to all orders in the strong field E_0 while keeping only first-order terms in the weak fields $E_{\pm 1}$. Within this approximation, the solutions to Eqs. (1) are found by considering the Floquet harmonic expansion: $\sigma^N = \sigma_0^N + \sigma_1^N \exp(-i\delta t) + \sigma_{-1}^N \exp(i\delta t)$ and $Z^N = Z_{dc}^N + Z_1^N \exp(-i\delta t)$ + c.c. [12]:

$$\begin{aligned}
\sigma_1^N &= \frac{dT_2}{\hbar(\xi + \Delta^N + i)}(E_1 Z_{dc}^N + E_0 Z_1^N),\\
\sigma_{-1}^{N*} &= \frac{-dT_2}{\hbar(\xi - \Delta^N + i)}(E_0^* Z_1^N + E_{-1}^* Z_{dc}^N),\\
Z_1^N &= \frac{-2dT_2}{\hbar(\xi + ir)}(E_0 \sigma_{-1}^{N*} + E_1 \sigma_0^{N*})\\
&\quad + \frac{2dT_2}{\hbar(\xi + ir)}(E_0^* \sigma_1^N + E_{-1}^* \sigma_0^N),
\end{aligned} \tag{4}$$

where $\xi = \delta T_2$ and $r = T_2/T_1$. The dc response of the population is Z_{dc}, and Z_1 accounts for the coherent population oscillations, which leads to the absorption dip.

We will refer to the Rabi frequency defined in units of $1/T_2$ as $\Omega_{0,\pm 1} = 2dE_{0,\pm 1}T_2/\hbar$ from now on as

$$\Omega_{0,\pm 1} = \Omega_{0,\pm 1}^{\text{in}} + i2\gamma_R \sum_N p(N)\sigma_{0,\pm 1}^N. \tag{5}$$

Here $\gamma_R = \mu_0 |d|^2 N_0 c\omega L T_2/2\hbar$ is the collective superradiant damping of an ensemble of two-level molecules.

Once we algebraically solve Eqs. (4) and take into account Eqs. (5), it can be demonstrated that

$$\frac{\Omega_0}{\Omega_0^{\text{in}}} = \left[1 + \frac{\gamma_R \sum_N p(N)(1 + i\Delta^N)}{1 + (\Delta^N)^2 + |\Omega_0|^2 r^{-1}}\right]^{-1}, \tag{6}$$

$$\begin{aligned}
\frac{\Omega_1}{\Omega_1^{\text{in}}} &= \left[1 + i\gamma_R \frac{\Omega_0^2 \Omega_{-1}^* (\xi + 2i)}{2\Omega_1^{\text{in}}} \sum_N \frac{p(N) Z_{\text{dc}}^N}{D^N(\Delta^N + i)}\right]\\
&\quad \times \left[1 - i\gamma_R(\xi + ir)\sum_N \frac{p(N) Z_{\text{dc}}^N (\xi - \Delta^N + i)}{D^N}\right.\\
&\quad \left. + i\gamma_R \frac{|\Omega_0|^2 \xi}{2} \sum_N \frac{p(N) Z_{\text{dc}}^N}{D^N(\Delta^N - i)}\right]^{-1},
\end{aligned} \tag{7}$$

$$\begin{aligned}
\frac{\Omega_{-1}^*}{\Omega_{-1}^{\text{in}*}} &= \left[1 + i\gamma_R \frac{\Omega_0^{*2} \Omega_1 (\xi + 2i)}{2\Omega_{-1}^{\text{in}*}} \sum_N \frac{p(N) Z_{\text{dc}}^N}{D^N(\Delta^N - i)}\right]\\
&\quad \times \left[1 - i\gamma_R(\xi + ir)\sum_N \frac{p(N) Z_{\text{dc}}^N (\xi + \Delta^N + i)}{D^N}\right.\\
&\quad \left. - i\gamma_R \frac{|\Omega_0|^2 \xi}{2} \sum_N \frac{p(N) Z_{\text{dc}}^N}{D^N(\Delta^N + i)}\right]^{-1},
\end{aligned} \tag{8}$$

where $D^N = (\xi + ir)(\xi + \Delta^N + i)(\xi - \Delta^N + i) - |\Omega_0|^2(\xi + i)$. Equation (6) has one or three roots depending on the parameters. This leads to bistable solutions for the strong field Ω_0 when γ_R is larger than a threshold value [7].

We consider an incident field such that $\Omega_1^{\text{in}} = \Omega_{-1}^{\text{in}*}$, leading to a sinusoidally modulated intensity with frequency δ. Thus, Eqs. (7) and (8) can be simplified, and the resulting fields fulfill $\Omega_1 = \Omega_{-1}^*$. The transmittance T and the dephasing ϕ induced by the film is calculated by the ratio between the output and the input signals:

$$\frac{\Omega_1 + \Omega_{-1}}{\Omega_1^{\text{in}} + \Omega_{-1}^{\text{in}}} = Te^{i\phi}. \tag{9}$$

Thus, the fractional delay is defined as $F = \phi/2\pi$.

We first analyze the case in the absence of size dispersion. We take the parameters of pseudoisocyanine-Br as it is one of the most studied J aggregates. Hence, we use $T_1 = 37$ ps (corresponding to a homogeneous aggregate of size $N = 100$) and $T_2 = 0.02T_1$. This value is consistent with measurements at low temperatures [13] and allows direct comparison with previous CPO works [14]. The transition dipole moment is $d^1 = 12.1$ D, and the concentration of aggregates is $N_0 \sim 10^{23}$ m^{-3}. These parameters give values for γ_R around 10 for film lengths of tens of nanometers. As in the usual CPO case, the maximum delay is obtained when the pump field reaches the saturation intensity, which depends on γ_R. Hereafter, and for each case shown, we will restrict ourselves to this optimal intensity. These values correspond to a photon flux of $\sim 1.4 \times 10^{11}$ photons/cm^2 for a 100-ps-length pulse and a surface density of monomers $\sim 10^{13}$ cm^{-2}. This means that the typical number of absorption and reemission cycles per aggregate is ~ 1, a much smaller value than those usually occurring in J-aggregate experiments [15], and that allows us to ensure photostability of the samples. Moreover, these intensities are low enough to neglect the blueshifted one-to-two exciton transitions, which supports the use of a two-level model [7].

Figure 1 shows the fractional delay and transmittance, calculated with Eq. (9), as a function of the normalized modulation frequency and for different values of γ_R. An increasing value of this parameter, which accounts for the collective interactions within the aggregate, gives rise to higher fractional delays reaching values of ~ 0.2 for $\gamma_R \sim 8$. Values of $\gamma_R > 8$ allow bistability to appear, which introduces a large signal distortion. Therefore, only cases up to $\gamma_R = 10$ are shown. Figure 1 (right panel) shows how the transmission increases with γ_R as well. It must be noted that the system presents gain ($T > 1$) in the weak probe electric fields for modulation frequencies close to those revealing the maximum fractional delay. We explain this behavior as a strong scattering process from the pump to the weak field due to the transient temporal grating generated in CPO. This is clearly relevant as CPO processes in other media usually present nondesirable residual absorption. Hence, in such cases it may be necessary to amplify the signal after propagation through the slow-light medium, especially for long media or high ion-densities [16]. The presence of gain in these films could overcome this drawback of CPO-based slow light while it is revealed as a clear difference with saturable absorption processes in typical two-level media.

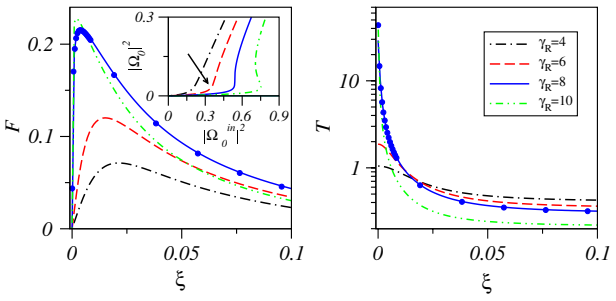

FIG. 1 (color online). Fractional delay and transmittance of a sinusoidal input signal as a function of the dimensionless detuning $\xi = \delta T_2$ for different values of γ_R and $G = 0$. The inset shows the output-input curve for the strong field Ω_0^2. The arrow points the optimal intensity for the case $\gamma_R = 6$. Solid dots result from numerical integration of Eqs. (1) and (2).

More relevant to telecommunication applications is the performance of the system with input-pulse signals. To analyze the fractional delay and distortion of the output pulses after passing through the ultrathin film, we numerically integrate Eqs. (1) together with Eq. (2). To validate the simulations, we first check the numerical integration with the results previously obtained. Figure 1 shows perfect agreement with the analytical predictions for the case of a sinusoidal input signal. Figure 2 depicts the fractional delay (F) and distortion (D) as a function of the pulse temporal width (defined as FWHM). The distortion is defined as the ratio between the output- and input-pulse standard deviations. Although the maximum fractional delay is accompanied by a large distortion, values up to $F = 0.33$ are obtained with distortion 2 for 135-ps-long pulses, which gives an ~ 7.5-GHz bandwidth. These results notably improve previous data obtained by CPO-based slow light in semiconductor materials at gigahertz bandwidths [17]. As mentioned before, increasing values of γ_R lead to larger delays. However, the distortion generated when bistability occurs limits in practice the values of γ_R up to 8 for $G = 0$ (no size dispersion). Note in Fig. 2 (inset) how the transmittance of the electric field is larger than 1 for most of the analyzed input-pulse widths, in agreement with the results of Fig. 1.

Let us now analyze the influence of the size dispersion on the slow-light performance. To numerically integrate Eqs. (1) and (2) with the inclusion of the inhomogeneous broadening, we carefully choose the sampling under the curve defined by Eq. (3) to reproduce the analytical results for a sinusoidal signal. We now focus on the effects of size dispersion on pulse propagation. As is well known, the presence of inhomogeneous broadening reduces the slow-light performance, as can be seen in Fig. 3, where the fractional delay and distortion are plotted against the

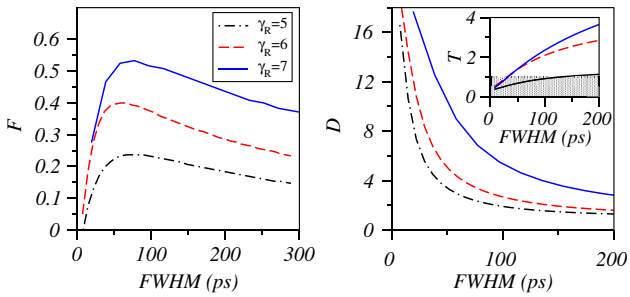

FIG. 2 (color online). Fractional delay and distortion for pulsed input signals against the initial pulse temporal width. Different values of γ_R are considered. Inset: Transmission vs FWHM.

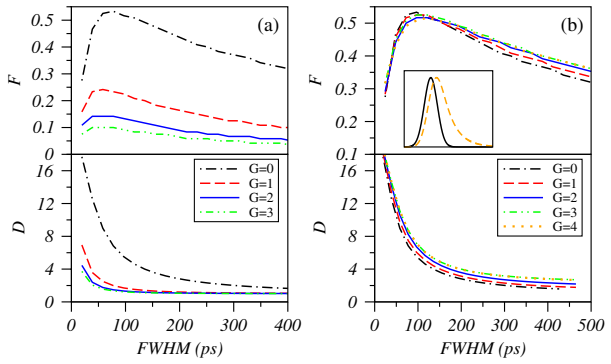

FIG. 3 (color online). Fractional delay and distortion for input pulses vs the initial pulse temporal width (FWHM), for different values of G and (a) $\gamma_R = 7$, (b) $\gamma_R = 7$ ($G = 0$), $\gamma_R = 12$ ($G = 1$), $\gamma_R = 22$ ($G = 2$), $\gamma_R = 34$ ($G = 3$), and $\gamma_R = 49$ ($G = 4$).

input-pulse width. A value of $G = 3$ already reduces the fractional delay up to 5 times with respect to the value obtained without size dispersion. However, as shown in the right panels of Fig. 3, the detrimental effect of a larger inhomogeneous linewidth can be compensated by increasing the value of γ_R. Larger values of γ_R can be obtained by modifying the temperature or increasing the aggregate concentration in the sample [7].

We finally propose a mechanism to take advantage of the optical bistability present in J-aggregate nanofilms for slow-light applications. Bistability allows us to rapidly change between two different output intensities for the same input. As the fractional delay depends on $|\Omega_0|^2$, this property turns out into a switch between two well-differentiated delays and distortions for the same $|\Omega_0^{\text{in}}|^2$. Figure 4 depicts this process for a value of $\gamma_R = 10$ and no size dispersion, where the bistability loop can be found for $0.69 \leq (\Omega_0^{\text{in}})^2 \leq 0.76$. Starting in the lower branch of the loop [position (1) in Fig. 4], and after propagating the first pulse, a short pulse in the input signal causes the system to switch to position (2), in the upper branch. Fractional delays achieved in positions (1) and (2), for a 111-ps-length pulse are 0.43 and 0.09, respectively, while the distortion values are 3.6 and 1.07. The lowest switching time is limited by T_1, according to simulations, being of some tens of picoseconds for J-aggregate films.

In conclusion, we showed that J-aggregate ultrathin films can produce large fractional delays by means of CPO processes, even in the presence of inhomogeneous broadening and thanks to the cooperative behavior of the aggregate molecules. This system does not suffer from residual absorption in the weak probe fields, in opposition to the usual CPO-based slow light. We also demonstrated how optical bistability could be used to produce a fast switch between different delays. We believe these organic compounds present a viable alternative to semiconductor slow-light devices in the nanoscale. To this end, our results can motivate further research at room-temperature operation and telecommunication bands. In this sense, the development of new aggregates such as porphocyanines

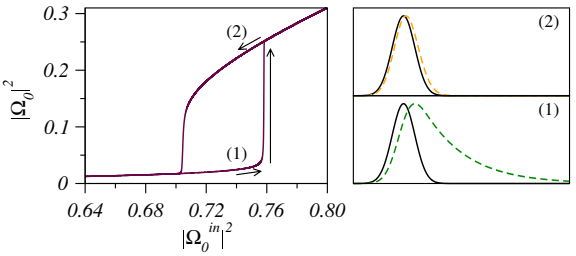

FIG. 4 (color online). Switch between different delays through the bistability loop for a pulse FWHM = 111 ps. Arrows mark the change of $|\Omega_0^2|$ when applying a short pulse in the input signal. In position (1) $F = 0.43$, while $F = 0.09$ in (2). Output and input pulses in (1) and (2) are shown in the right panel.

[18] provides great opportunities. Moreover, new studies including processes such as one-to-two exciton transitions and exciton-exciton annihilation are currently in progress. These effects seems to counteract the killing action of the inhomogeneous broadening [19], which would impose better experimental conditions to obtain the delays shown in this work.

This work was supported by projects MOSAICO, No. MAT2010-17180, and No. CCG08-UCM/ESP-4330. E. D. acknowledges financial support by Ministerio de Eduacion y Ciencia. O. G. C. acknowledges support from project FIS2010-22082 (MEC). We thank A. Eisfeld for valuable discussions.

[1] *Slow Light: Science and Applications*, edited by B. Khurgin and R. S. Tucker (CRC, Boca Raton, FL, 2008).
[2] R. W. Boyd and D. J. Gauthier, Science **326**, 1074 (2009).
[3] G. M. Gehring *et al.*, J. Lightwave Technol. **26**, 3752 (2008);
[4] Matthew S. Bigelow, Nick N. Lepeshkin, and Robert W. Boyd, Phys. Rev. Lett. **90**, 113903 (2003).
[5] V. S. Zapasskii and G. G. Kozlov, Opt. Express **17**, 22 154 (2009).
[6] A. C. Selden, Opt. Spectrosc. **106**, 881 (2009).
[7] Victor A. Malyshev *et al.*, J. Chem. Phys. **113**, 1170 (2000).
[8] Jasper Knoester, Int. J. Photoenergy **2006**, 61364 (2006).
[9] V. A. Malyshev and Enrique Conejero Jarque, Opt. Express **6**, 227 (2000).
[10] V. V. Shelkovnikov, J. Appl. Spectrosc. **76**, 66 (2009).
[11] Zhien Lu and Ka-Di Zhu, J. Phys. B **42**, 015502 (2009).
[12] D. J. Harter and R. W. Boyd, IEEE J. Quantum Electron. **16**, 1126 (1980).
[13] Henk Fidder *et al.*, Chem. Phys. Lett. **171**, 529 (1990).
[14] R. W. Boyd *et al.*, Phys. Rev. A **24**, 411 (1981).
[15] R. V. Markova, A. I. Plekhanov, V. V. Shelkovnikov, and J. Knoester, Microelectron. Eng. **69**, 528 (2003).
[16] Sonia Melle *et al.*, Opt. Commun. **279**, 53 (2007).
[17] Phedon Palinginis *et al.*, Appl. Phys. Lett. **87**, 171102 (2005).
[18] Joel M. Hales *et al.*, in *Proceedings of IEEE 2009 OSA/CLEO/IQEC* (IEEE, New York, 2009).
[19] H. Glaeske *et al.*, J. Chem. Phys. **114**, 1966 (2001).